Pharmacological Research 137 (2018) 47–55

Contents lists available at ScienceDirect

Pharmacological Research

journal homepage: www.elsevier.com/locate/yphrs

P-glycoprotein and breast cancer resistance protein restrict brigatinib brain accumulation and toxicity, and, alongside CYP3A, limit its oral availability

Wenlong Li[a], Rolf W. Sparidans[b], Yaogeng Wang[a], Maria C. Lebre[a], Jos H. Beijnen[a,b,c], Alfred H. Schinkel[a,*]

[a] The Netherlands Cancer Institute, Division of Pharmacology, Plesmanlaan 121, 1066 CX Amsterdam, the Netherlands
[b] Utrecht University, Faculty of Science, Department of Pharmaceutical Sciences, Division of Pharmacoepidemiology & Clinical Pharmacology, Universiteitsweg 99, 3584 CG, Utrecht, the Netherlands
[c] Medical Center Slotervaart, Department of Pharmacy & Pharmacology, Plesmanlaan 121, 1066 CX, Amsterdam, the Netherlands

ARTICLE INFO

Chemical compounds studied in this article:
Brigatinib (CID: 68165256)
Elacridar HCl (CID: 170320)
Ko143 (CID: 10322450)
Zosuquidar trihydrochloride (CID: 153997)

Keywords:
Brigatinib
P-glycoprotein
Brain accumulation
Cytochrome P450-3A
Oral availability

ABSTRACT

Brigatinib is an FDA-approved oral anaplastic lymphoma kinase (ALK) inhibitor for treatment of metastatic non-small cell lung cancer (NSCLC). Using genetically modified mouse models, we investigated the roles of the multidrug efflux transporters ABCB1 and ABCG2, and the multispecific drug-metabolizing enzyme CYP3 A in plasma pharmacokinetics and tissue distribution of brigatinib. *In vitro*, brigatinib was exceptionally well transported by human ABCB1 and mouse Abcg2, and efficiently by human ABCG2. Following oral brigatinib administration (10 mg/kg), brain accumulation was dramatically increased in *Abcb1a/1b*$^{-/-}$ (19.3-fold) and *Abcb1a/1b;Abcg2*$^{-/-}$(41.8-fold), but not in single *Abcg2*$^{-/-}$ mice compared to wild-type mice. Brigatinib testis accumulation showed qualitatively similar behavior. mAbcb1a/1b and mAbcg2 together restricted systemic exposure of brigatinib: with both systems absent oral availability increased 1.9-fold. Coadministration of elacridar, an ABCB1/ABCG2 inhibitor, caused a pronounced increase (36-fold) in brain-to-plasma ratios of brigatinib, approaching the levels seen in *Abcb1a/1b;Abcg2*$^{-/-}$ mice. Unexpectedly, lethal toxicity of oral brigatinib was observed in mice with genetic knockout or pharmacological inhibition of mAbcb1a/1b and mAbcg2, indicating a pronounced protective role for these transporters. In *Cyp3a*$^{-/-}$ mice, brigatinib plasma exposure increased 1.3-fold, and was subsequently 1.8-fold reduced by transgenic overexpression of human CYP3 A4 in liver and intestine. The relative tissue distribution of brigatinib, however, remained unaltered. ABCB1 and ABCG2 thus limit brain accumulation, toxicity, and systemic exposure of brigatinib, whereas CYP3 A also markedly restricts its oral availability. Unexpected toxicities should therefore be carefully monitored when brigatinib is coadministered with ABCB1/ABCG2 inhibitors in patients. Collectively, these insights may support the clinical application of brigatinib.

1. Introduction

Lung cancer remains the leading cause of cancer deaths in the world [1]. The majority of lung cancers are non-small cell lung cancers (NSCLCs), in ~5% of which anaplastic lymphoma kinase (ALK) gene rearrangements are present [2]. The recent development of highly potent targeted drugs has resulted in marked therapeutic advances in management of patients with ALK-positive NSCLC. Crizotinib was the first ALK inhibitor with significant benefits over chemotherapy to be approved by the US Food and Drug Administration (FDA) in 2011 [3]. However, most patients develop disease progression especially in the central nervous system (CNS) and acquire resistance to crizotinib [4,5].

Abbreviations: ABC, ATP-binding cassette; ALK, anaplastic lymphoma kinase; ANOVA, analysis of variance; AUC, area under plasma concentration-time curve; BBB, blood-brain barrier; BCRP, breast cancer resistance protein; BTB, blood-testis barrier; C_{brain}, brain concentration; C_{max}, maximum drug concentration in plasma; C_{testis}, testis concentration; CNS, central nervous system; CYP, cytochrome P450; Cyp3a$^{-/-}$, Cyp3a knockout mice; Cyp3aXAV, Cyp3a knockout mice with specific expression of human CYP3 A4 in liver and intestine; h (as prefix), human; LC–MS/MS, liquid chromatography coupled with tandem mass spectrometry; MDCK, Madin-Darby canine kidney; m (as prefix), mouse; NSCLC, non-small cell lung cancer; P_{brain}, relative brain accumulation; P_{testis}, relative testis accumulation; P-gp, P-glycoprotein; SD, standard deviation; TKI, tyrosine kinase inhibitor; T_{max}, time to reach maximum drug concentration in plasma

* Corresponding author at: Division of Pharmacology, The Netherlands Cancer Institute, Plesmanlaan 121, 1066 CX, Amsterdam, the Netherlands.
E-mail address: a.schinkel@nki.nl (A.H. Schinkel).

https://doi.org/10.1016/j.phrs.2018.09.020
Received 7 July 2018; Received in revised form 14 September 2018; Accepted 20 September 2018
Available online 22 September 2018

Classically, second-generation ALK inhibitors such as alectinib and ceritinib have been the standard of care in crizotinib-resistant patients [6,7]. However, each drug has a different spectrum of sensitivity to ALK mutations, complicating the optimal treatment strategy for the resistant population.

Brigatinib (AP26113, Alunbrig), the third second-generation ALK inhibitor, is a pyrimidine-based molecule containing a C4 aniline with an ortho-dimethylphosphine oxide substituent [8] (Supplemental Fig. 1). This unique structural feature, a novel hydrogen bond acceptor, is critical for balancing ALK potency and selectivity over the highly homologous IGF-1R and ISNR kinases. Moreover, the highly ionic P═O bond imparts brigatinib with important drug-like properties, including decreased lipophilicity, increased aqueous solubility, reduced protein binding, and robust metabolic stability [8].

Preclinical data show that brigatinib is active *in vitro* against many ALK kinase domain mutations including L1196 M, E1210 K, and G1202R which may mediate acquired resistance to other ALK inhibitors [9]. Brigatinib showed promising activity in ALK-rearranged NSCLC that had previously received crizotinib, with response rates ranging from 42 to 50%, intracranial responses 42–63%, and median progression-free survival of 9.2–12.9 months [10]. It has an acceptable safety profile, but early pulmonary toxicity has been observed, promoting daily dosing of 180 mg (with 7-day lead-in at 90 mg), which is also the recommended dosage in the clinic [10,11]. Brigatinib has been approved by the FDA for ALK-positive NSCLC patients who are resistant to prior crizotinib. A randomized Phase III trial of brigatinib versus crizotinib in ALK inhibitor-naïve patients is currently running (NCT02737501).

ATP-binding cassette (ABC) drug efflux transporters, such as P-glycoprotein (P-gp/MDR1/ABCB1) and breast cancer resistance protein (BCRP/ABCG2) are expressed on the apical membrane of epithelia in a number of organs essential for absorption and elimination of drugs like the liver, small intestine and kidneys, but also on luminal membranes of barriers protecting sanctuary tissues like the blood-brain barrier (BBB), blood-testis barrier (BTB) and blood-placenta barrier, as well as in a number of tumors [12–14]. ABCB1 or ABCG2 transport substrates are immediately pumped out of the cell back into blood, resulting in limited therapeutic efficacy of drugs due to lower accumulation in these sanctuary sites [15–17]. Brain metastasis for instance is a major clinical problem in the treatment of advanced NSCLC, since brain penetration of most currently available systemic drugs is restricted by ABC transporters in the BBB [18,19]. Many tyrosine kinase inhibitors (TKIs) have been shown to be transported by ABCB1 and/or ABCG2, often resulting in decreased brain accumulation and/or oral availability [15–17]. According to the manufacturer, brigatinib is a substrate for P-gp and BCRP *in vitro* [20]. However, the relative roles of Abcb1 and Abcg2 in restricting brain accumulation and oral availability of brigatinib remain unknown.

Cytochromes P450 (CYPs) are major enzyme families accounting for about 75% of the total drug metabolism [21]. Brigatinib is primarily metabolized by CYP2C8 and CYP3 A4 *in vitro*. Steady-state plasma exposure of its primary metabolite, AP26123, was less than 10% of brigatinib exposure in patients. AP26123 also inhibited ALK with ~4-fold lower efficacy than brigatinib *in vitro* [20]. The metabolite is thus less relevant than brigatinib in inhibition of ALK. Although brigatinib is metabolized by CYP3 A4 *in vitro*, the extent of interaction of CYP3 A with brigatinib *in vivo* is still unclear. To what extent CYP3 A affects plasma exposure and oral availability of brigatinib, and even therapeutic efficacy, should therefore be further studied.

We here studied the interaction of brigatinib with the ABC transporters ABCB1 and ABCG2 *in vitro* as well as *in vivo*, using genetically modified cell lines and mouse models, and pharmacological inhibition of ABCB1 and ABCG2. We also investigated to what extent CYP3 A impacts oral availability of brigatinib *in vivo*.

2. Materials and methods

2.1. Chemicals

Brigatinib was purchased from MedChem Express (Middlesex County, USA). Zosuquidar trihydrochloride and elacridar HCl were obtained from Sequoia Research Products (Pangbourne, United Kingdom). Ko143 was from Tocris Bioscience (Bristol, United Kingdom). Bovine Serum Albumin (BSA) Fraction V was obtained from Roche Diagnostics (Mannheim, Germany). Glucose water (5%, w/v) was from B. Braun Medical Supplies, Inc. (Melsungen, Germany). Isoflurane was purchased from Pharmachemie (Haarlem, The Netherlands), heparin (5000 IU ml^{-1}) was from Leo Pharma (Breda, The Netherlands). All other chemicals and reagents were obtained from Sigma-Aldrich (Steinheim, Germany).

2.2. Cell lines and transport assays

Madin-Darby Canine Kidney (MDCK-II) cells (ECACC 00062107) stably transduced with human (h) ABCB1, hABCG2, or mouse (m) Abcg2 cDNA were generated in our institute between 1998-2005. These polarized epithelial cells show highly characteristic growth and transport properties, including inhibitor sensitivity, confirming their proper identity [22,23]. Cells were routinely tested negative for mycoplasma. The passage number when used in transport experiments was 10–15.

Transepithelial transport experiments in these cell lines were performed as previously described [17]. Where appropriate 5 μM zosuquidar (ABCB1 inhibitor) and/or 5 μM Ko143 (ABCG2/Abcg2 inhibitor) were used during the transport experiments, after pre-incubation with these inhibitors for 1 h in both compartments. The transport phase was started (t = 0) by replacing the medium in the apical or basolateral compartment with fresh DMEM including 10% (v/v) fetal bovine serum (FBS) and brigatinib at 5 μM, as well as the appropriate inhibitor(s). Cells were kept at 37 °C in 5% CO_2 during the experiment, and 50 μl aliquots were taken from the acceptor compartment at 1, 2, 4 and 8 h, and stored at −30 °C until LC–MS/MS measurement of the concentrations of brigatinib. Active transport was expressed using the transport ratio r, i.e., the amount of apically directed drug transport divided by basolaterally directed drug translocation after 8 h.

2.3. Animals

Mice were housed and handled according to institutional guidelines complying with Dutch and EU legislation. Male wild-type, *Abcb1a/1b*$^{-/-}$, *Abcg2*$^{-/-}$, *Abcb1a/1b;Abcg2*$^{-/-}$, *Cyp3a*$^{-/-}$ and Cyp3aXAV mice, all of a > 99% FVB genetic background, were used between 10 and 15 weeks of age. Animals were kept in a temperature-controlled environment with a 12-h light and 12-h dark cycle and they received a standard diet (Transbreed, SDS Diets, Technilab − BMI, Someren, The Netherlands) and acidified water *ad libitum*.

2.4. Drug solutions

For oral administration, brigatinib was dissolved in 25 mM sodium citrate buffer (pH 4.5) to yield a concentration of 0.5, 1 or 2.5 mg/ml. Elacridar hydrochloride was dissolved in DMSO (53 mg/ml) in order to get 50 mg pure elacridar per ml DMSO. The stock solution was further diluted with a mixture of polysorbate 80, ethanol and water [20:13:67, (v/v/v)] to yield a concentration of 5 mg/ml elacridar, and orally administered at a dose of 50 mg/kg body weight. All dosing solutions were prepared freshly on the day of experiment.

2.5. Plasma pharmacokinetics and organ accumulation of brigatinib in mice

To minimize variation in absorption upon oral administration, mice were fasted for 3 h before brigatinib was administered by gavage into

the stomach, using a blunt-ended needle. For the 24 h or 8 h experiments, tail vein blood sampling was performed at 0.5, 1, 2, 4, and 8 h or 0.25, 0.5, 1, 2, and 4 h time points after oral administration, respectively, using microvettes containing heparin. Twenty-four or eight hours after oral administration (25 mg/kg or 10 mg/kg), mice were anesthetized with isoflurane and blood was collected by cardiac puncture. Blood samples were collected in Eppendorf tubes containing heparin as an anticoagulant. The mice were then sacrificed by cervical dislocation and brain, liver, spleen, kidneys, lung, small intestine, and testis were rapidly removed. The contents of the small intestine were removed, and the tissue quickly rinsed with saline before homogenization of the tissue. Organs were homogenized with 4% (w/v) bovine serum albumin. Plasma was isolated from the blood by centrifugation at 9 000 × g for 6 min at 4 °C, and the plasma fraction was collected. All samples were stored at −30 °C until analysis. Relative tissue accumulation after oral administration was calculated by determining brigatinib tissue concentration at 24 h or 8 h relative to plasma $AUC_{0\text{-}24h}$ or $AUC_{0\text{-}8h}$.

2.6. Brain accumulation of brigatinib in combination with oral elacridar

Wild-type and *Abcb1a/1b;Abcg2*$^{-/-}$ mice were fasted for 3 h before oral administration of either elacridar (50 mg/kg) or vehicle. Fifteen minutes later, brigatinib (5 mg/kg) was administered to mice orally. Tail vein blood sampling was performed at 7.5 min, 15 min, 30 min, 1 h and 2 h time points after brigatinib administration. Blood, brain, liver, lung, small intestine, and testis were isolated at the 4 h time point, and processed as described above. Tissue-to-plasma ratios at t = 4 h were calculated per individual mouse by dividing the tissue concentration by the corresponding plasma concentration.

2.7. LC–MS/MS analysis

Brigatinib concentrations in DMEM cell culture medium, plasma samples, and organ homogenates were determined using a sensitive and specific liquid chromatography-tandem mass spectrometry assay [24].

2.8. Pharmacokinetic calculations and statistical analysis

Pharmacokinetic parameters were calculated by non-compartmental methods using the software GraphPad Prism 7 (GraphPad Software, La Jolla, CA, USA). The area under the plasma concentration-time curve (AUC) was calculated using the trapezoidal rule, without extrapolating to infinity. The peak plasma concentration (C_{max}) and the time of maximum plasma concentration (T_{max}) were estimated from the original data. One-way analysis of variance (ANOVA) was used when multiple groups were compared and the Bonferroni *post hoc* correction was used to accommodate multiple testing. The two-sided unpaired Student's *t*-test was used when treatments or differences between two groups were compared. Differences were considered statistically significant when $P < 0.05$. All data are presented as geometric mean ± SD.

3. Results

3.1. In vitro transport of brigatinib

Transepithelial brigatinib transport was tested using polarized monolayers of Madin-Darby Canine Kidney (MDCK-II) parental cells and its subclones overexpressing hABCB1, hABCG2, or mAbcg2. Brigatinib (5 μM) was modestly transported in the apical direction in the parental MDCK-II cell line (r = 2.70, Fig. 1A), which was clearly reduced by addition of the ABCB1 inhibitor zosuquidar (r = 1.37, Fig. 1B). These data are compatible with modest transport of brigatinib by the low-level endogenous canine ABCB1. In cells overexpressing hABCB1, there was very strong apically directed transport of brigatinib (r = 24.3, Fig. 1C), which was extensively inhibited by zosuquidar (r = 1.56, Fig. 1D).

In subsequent experiments with MDCK-II cells overexpressing hABCG2 and mAbcg2, zosuquidar was added to inhibit any possible contribution of endogenous canine ABCB1. Brigatinib was actively transported by cells overexpressing hABCG2 and mAbcg2, with transport ratios of 2.19 (Fig. 1E) and 13.1 (Fig. 1G), respectively, versus 1.37 in parental cells. The addition of Ko143, a specific ABCG2 inhibitor, resulted in extensive inhibition of the transport activity of hABCG2 and mAbcg2 (Fig. 1F and H). In summary, brigatinib appears to be very efficiently transported by hABCB1 and mABCG2, and modestly by hABCG2 and canine ABCB1. However, even with zosuquidar and/or Ko143, some apical transport was still detectable (Fig. 1B, D, F, and H, r ≥ 1.37). This suggests that some other brigatinib efflux system may exist in MDCK-II cells.

3.2. Impact of ABCB1 and ABCG2 on brigatinib plasma pharmacokinetics and tissue disposition

To assess the possible impact of mAbcb1a/1b and mAbcg2 on oral availability and tissue disposition of brigatinib, we performed a 24-h pilot study in male wild-type and combination *Abcb1a/1b;Abcg2*$^{-/-}$ mice. Based on the literature [9], in order to obtain plasma levels of brigatinib in mice similar to steady-state therapeutic plasma concentrations in patients, we dosed brigatinib orally at 25 mg/kg. As shown in Supplemental Fig. 2 and Supplemental Table 1, plasma exposure of brigatinib over 24 h ($AUC_{0\text{-}24h}$) was significantly higher (1.3-fold) in *Abcb1a/1b;Abcg2*$^{-/-}$ mice compared to wild-type mice. The plasma elimination of brigatinib was markedly delayed in the *Abcb1a/1b;Abcg2*$^{-/-}$ mice, especially beyond 4–8 h after oral administration (Supplemental Fig. 2B).

Brain, liver, spleen, kidney, lung, small intestinal tissue, and testis concentrations of brigatinib were also measured 24 h after oral administration. We observed dramatic increases in brain concentration (388-fold) and brain-to-plasma ratio (52-fold) in *Abcb1a/1b;Abcg2*$^{-/-}$ mice compared to wild-type mice (Supplemental Fig. 3; Supplemental Table 1). In contrast, exposure of brigatinib in other organs was not much altered when considering the tissue-to-plasma ratios, except for lung and small intestinal tissue (Supplemental Fig. 4). The brain-to-plasma ratios of brigatinib in wild-type mice were around 0.12, indicating relatively low penetration of brigatinib into normal brain at this time point.

Interestingly, during the 24 h experiment, 4 out of 8 *Abcb1a/1b;Abcg2*$^{-/-}$ mice showed modest to severe toxicity signs, including hypoactivity, tonic convulsions, impaired equilibrium, increased respiration rate, and accumulation of red material around the nose and mouth. Two *Abcb1a/1b;Abcg2*$^{-/-}$ mice even died around 8 h after drug administration. In contrast, no toxicity signs were observed in wild-type mice. Retrospective analysis of the individual plasma pharmacokinetics in the 6 surviving *Abcb1a/1b;Abcg2*$^{-/-}$ mice showed that all mice displayed delayed plasma clearance of brigatinib, regardless of the presence of toxicity signs.

To further investigate the separate and combined effects of mAbcb1a/1b and mAbcg2 on oral availability and tissue disposition of brigatinib, a more extensive experiment was performed up till 8 h, when plasma levels were still comparatively high. To avoid the severe toxicity for knockout mice, the dosage of brigatinib was reduced to 10 mg/kg. We administered brigatinib orally to male wild-type, *Abcb1a/1b*$^{-/-}$, *Abcg2*$^{-/-}$, and *Abcb1a/1b;Abcg2*$^{-/-}$ mice. As shown in Fig. 2A and Table 1, the T_{max} in *Abcb1a/1b*$^{-/-}$, *Abcg2*$^{-/-}$, and *Abcb1a/1b;Abcg2*$^{-/-}$ mice occurred somewhat earlier than in wild-type mice. Absence of either mAbcb1a/1b or mAbcg2 each resulted in a 1.2-fold increase in the plasma $AUC_{0\text{-}8h}$, but these changes were not statistically significant. However, combined deficiency in mAbcb1a/1b and mAbcg2 caused a 1.9-fold, highly significant increase in plasma $AUC_{0\text{-}8h}$ relative to wild-type mice (Fig. 2A; Table 1). These results

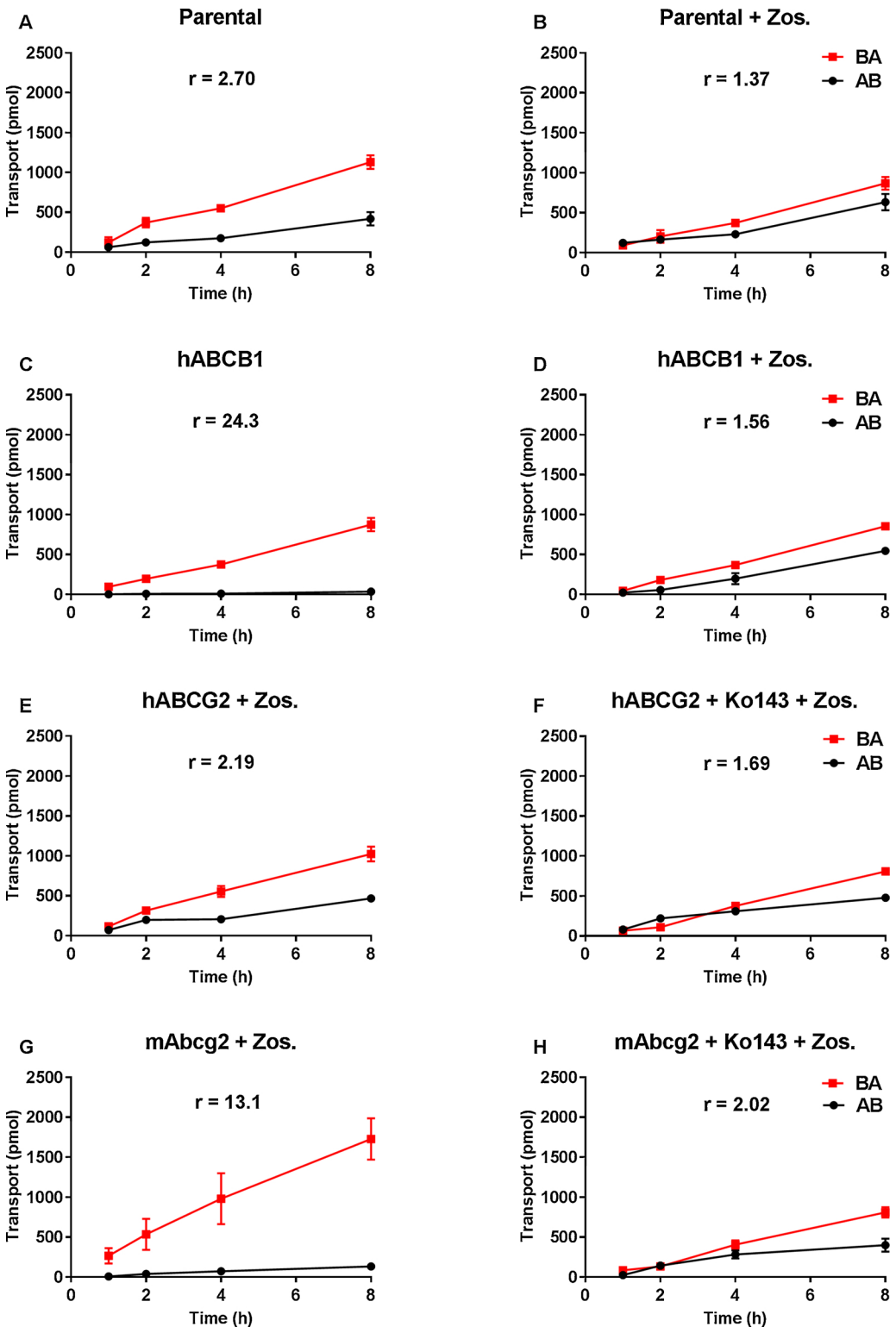

Fig. 1. Transepithelial transport of brigatinib (5 μM) assessed in MDCK-II cells either non-transduced (A, B), transduced with hABCB1 (C, D), hABCG2 (E, F) or mAbcg2 (G, H) cDNA. At t = 0 h, brigatinib was applied in the donor compartment and the concentrations in the acceptor compartment at t = 1, 2, 4, and 8 h were measured and plotted as brigatinib transport (pmol) in the graph (n = 3). B, D–H: Zos. (zosuquidar, 5 μM) was applied to inhibit human and/or endogenous canine ABCB1. F and H: the ABCG2 inhibitor Ko143 (5 μM) was applied to inhibit ABCG2/Abcg2–mediated transport. *r*, relative transport ratio. BA (■), translocation from the basolateral to the apical compartment; AB (●), translocation from the apical to the basolateral compartment. Points, mean; bars, S.D.

suggest that, at least at this brigatinib dose, mAbcb1a/1b and mAbcg2 each restrict systemic exposure of brigatinib, and only when both systems are absent oral availability is markedly increased.

At 8 h, the brigatinib brain concentrations were dramatically increased in *Abcb1a/1b*$^{-/-}$ mice and *Abcb1a/1b;Abcg2*$^{-/-}$ mice compared to wild-type mice, but not in single *Abcg2*$^{-/-}$ mice (Fig. 3A; Table 1). The brain-to-plasma ratios of brigatinib were relatively low (0.09) in wild-type mice, and these were substantially increased by 20.7-fold and 47.9-fold in *Abcb1a/1b*$^{-/-}$ and *Abcb1a/1b;Abcg2*$^{-/-}$ mice, respectively (Fig. 3B; Table 1), but not in single *Abcg2*$^{-/-}$ mice. Similar results were obtained for the brain accumulations (Fig. 3C; Table 1). These data indicate that mAbcb1 can profoundly restrict brain accumulation of brigatinib, whereas mAbcg2 also contributes to this process, although this can only be observed when mAbcb1 is absent.

As shown in Fig. 3E and Table 1, testis-to-plasma ratios were also substantially higher in *Abcb1a/1b*$^{-/-}$ (2.4-fold) and *Abcb1a/1b;Abcg2*$^{-/-}$ (3.5-fold) mice compared to wild-type mice, but not in single *Abcg2*$^{-/-}$ mice. The testis-to-plasma ratios of brigatinib were

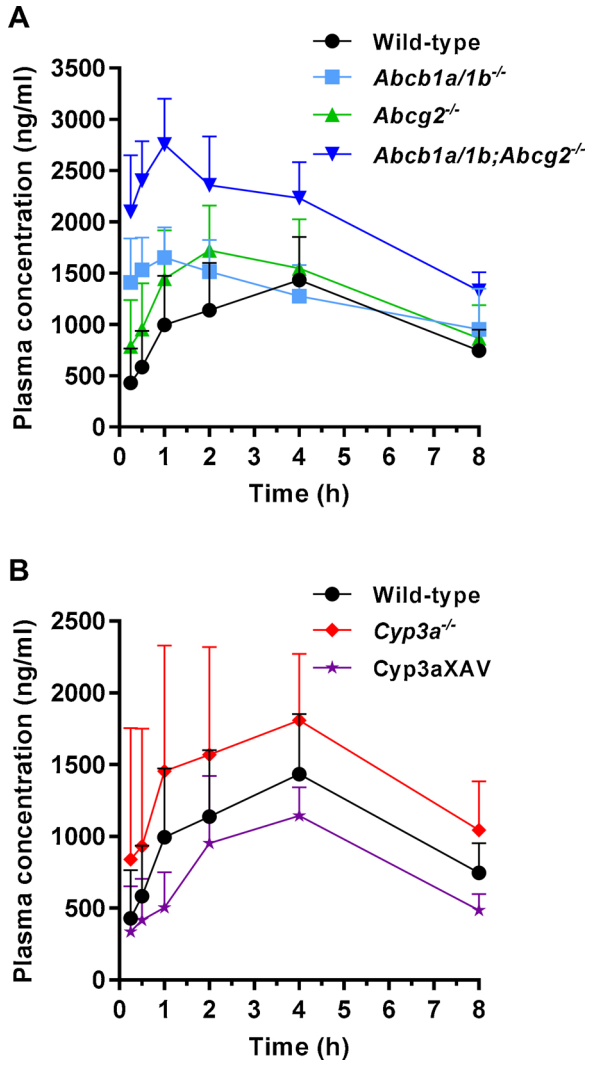

Fig. 2. Plasma concentration-time curves of brigatinib in male wild-type, *Abcb1a/1b*$^{-/-}$, *Abcg2*$^{-/-}$, *Abcb1a/1b;Abcg2*$^{-/-}$, *Cyp3a*$^{-/-}$, and Cyp3aXAV mice over 8 h after oral administration of 10 mg/kg brigatinib. Data are presented as mean ± S.D. (n = 6–9). Panel A: wild-type, *Abcb1a/1b*$^{-/-}$, *Abcg2*$^{-/-}$, and *Abcb1a/1b;Abcg2*$^{-/-}$ mice. Panel B: wild-type, *Cyp3a*$^{-/-}$ and Cyp3aXAV mice.

0.88 in wild-type mice, which is around 10-fold higher than that for brain, indicating a much higher intrinsic accessibility of testis for brigatinib, and the relative impact of mAbcb1a/1b and mAbcg2 deficiency was accordingly much lower.

In contrast to brain and testis, all other tested organs including liver, spleen, kidney, lung, and small intestinal tissue, demonstrated no meaningful differences in tissue concentrations, tissue-to-plasma ratios, or tissue accumulation of brigatinib between the mouse strains. Tissue-to-plasma distribution ratios were about 7.6, 15.0, 8.5, 6.0 and 7.5 for liver, spleen, kidney, lung and small intestinal tissue, respectively (Supplemental Figure 5), far higher than those observed for brain (0.09) and testis (0.88).

At this reduced brigatinib dose, similar but more modest signs of toxicity were observed in some *Abcb1a/1b*$^{-/-}$ and *Abcb1a/1b;Abcg2*$^{-/-}$ mice, including hypoactivity, tonic convulsions, increased respiration rate and the tendency to continuously touch the eyes. No mice died during this 8 h experiment.

3.3. Impact of CYP3 A on brigatinib plasma pharmacokinetics and tissue disposition

Brigatinib is primarily metabolized by CYP2C8 and CYP3 A *in vitro* [20]. To assess the interaction between brigatinib and CYP3 A *in vivo*, we performed a 24 h pilot experiment with oral brigatinib at 25 mg/kg in male wild-type and Cyp3a knockout (*Cyp3a*$^{-/-}$) mice. The oral plasma $AUC_{0\text{-}24h}$ in *Cyp3a*$^{-/-}$ mice was 1.5-fold higher ($P < 0.001$) than that in wild-type mice (Supplemental Fig. 2; Supplemental Table 1). However, the terminal elimination rate (between 8 and 24 h) was similar between the two strains. In contrast to the overall plasma exposure, the relative tissue disposition of brigatinib as judged by tissue-to-plasma ratio was not significantly different between wild-type and *Cyp3a*$^{-/-}$ mice (Supplemental Figs. 3 and 4; Supplemental Table 1), except for a borderline significant increase in small intestinal tissue (Supplemental Fig. 4M-O). Although the plasma AUC and C_{max} in *Cyp3a*$^{-/-}$ mice were at least as high as in *Abcb1a/1b;Abcg2*$^{-/-}$ mice (Supplemental Fig. 2; Supplemental Table 1), we did not observe any indication for toxicity. These data indicate that mCyp3a could limit brigatinib systematic exposure, but did not markedly affect tissue distribution or toxicity at a dosage of 25 mg/kg.

To clarify the impact of human CYP3 A4 on brigatinib pharmacokinetics, in a subsequent 8-h experiment we included male *Cyp3a*$^{-/-}$ mice with specific transgenic expression of human CYP3 A4 in liver and intestine (Cyp3aXAV mice). After oral administration of 10 mg/kg brigatinib to wild-type, *Cyp3a*$^{-/-}$ and Cyp3aXAV mice, blood and organs were collected. As shown in Fig. 2B and Table 1, the time to reach peak plasma concentrations was about 4 h in each strain. Because of the high interindividual variation, there was no significant difference between wild-type and *Cyp3a*$^{-/-}$ mice ($P = 0.063$), even though the oral $AUC_{0\text{-}8h}$ in *Cyp3a*$^{-/-}$ mice appeared 1.3-fold increased. Also no significant differences were observed between wild-type and Cyp3aXAV mice ($P = 0.079$). However, brigatinib plasma exposure in Cyp3aXAV mice was substantially decreased by 1.8-fold ($P < 0.01$) relative to *Cyp3a*$^{-/-}$ mice (Fig. 2B; Table 1). This clearly suggests that human CYP3 A4 plays an important role in brigatinib metabolism and oral availability. At the same time, no meaningful differences were observed in relative tissue distribution (tissue-to-plasma ratio) between wild-type, *Cyp3a*$^{-/-}$ and Cyp3aXAV mice (Supplemental Figure 5). Modest but sometimes statistically significant differences observed in this Supplemental figure may in part have to do with the large number of data compared.

Collectively, these results suggest that at a dosage of 10 mg/kg hCYP3 A4 could substantially restrict brigatinib plasma exposure. mCyp3a can play a detectable role in limiting brigatinib availability when the dosage was increased to 25 mg/kg. However, neither human CYP3 A4 nor mouse Cyp3a appears to have a noticeable effect on the relative brigatinib tissue distribution.

3.4. Effect of the dual ABCB1 and ABCG2 inhibitor elacridar on brigatinib plasma exposure and brain accumulation

As shown in Figs. 2 and 3, and Table 1, there are substantial differences between wild-type and Abcb1a/1b;Abcg2$^{-/-}$ mice in plasma exposure and brain accumulation. In view of the potential benefit of enhancing brigatinib brain accumulation, and possibly also plasma exposure, we wanted to investigate to what extent the dual ABCB1 and ABCG2 inhibitor elacridar could increase the oral availability and brain accumulation of brigatinib. To assess the effects around the T_{max}, and in order to avoid possible toxicity, we performed a 4-h experiment with a further reduced dose of brigatinib, as 10 mg/kg brigatinib still caused clear toxicity in some *Abcb1a/1b;Abcg2*$^{-/-}$ mice. Thus, we administered elacridar (50 mg/kg) orally 15 min prior to oral brigatinib (5 mg/kg) to

Table 1
Plasma, brain, and testis pharmacokinetic parameters of brigatinib 8 h after oral administration of 10 mg/kg brigatinib to male wild-type, *Abcb1a/1b*$^{-/-}$, *Abcg2*$^{-/-}$, *Abcb1a/1b;Abcg2*$^{-/-}$, *Cyp3a*$^{-/-}$, and Cyp3aXAV mice.

Parameter	Genotype					
	Wild-type	*Abcb1a/1b*$^{-/-}$	*Abcg2*$^{-/-}$	*Abcb1a/1b;Abcg2*$^{-/-}$	*Cyp3a*$^{-/-}$	Cyp3aXAV
$AUC_{0\text{-}8h}$, ng/ml.h	8573 ± 2559	10176 ± 2124	10636 ± 3064	16383 ± 2128***	11,523 ± 3372	6352 ± 1372^^
Fold change $AUC_{0\text{-}8h}$	1.0	1.2	1.2	1.9	1.3	0.7
C_{max}, ng/ml	1452 ± 430	1768 ± 361	1749 ± 454	2780 ± 464	2049 ± 558	1254 ± 326
T_{max}, h	4	1	2	1	4	4
C_{brain}, ng/g	69 ± 18	1622 ± 308***	105 ± 46	5638 ± 479***(###)	104 ± 29	57 ± 15
Fold change C_{brain}	1.0	23.5	1.5	81.7	1.5	0.8
Brain-to-plasma ratio	0.09 ± 0.02	1.86 ± 0.53***	0.13 ± 0.06	4.31 ± 0.64***(###)	0.11 ± 0.07	0.12 ± 0.02
Fold increase ratio	1.0	20.7	1.4	47.9	1.2	1.3
P_{brain} (*10^{-3} h^{-1})	8.3 ± 1.1	160.6 ± 17.0***	10.3 ± 4.7	346.7 ± 29.5***(###)	9.7 ± 4.1	9.1 ± 2.5
Fold increase P_{brain}	1.0	19.3	1.2	41.8	1.2	1.1
C_{testis}, ng/g	629 ± 184	1853 ± 508**	1073 ± 902	4108 ± 955***(###)	840 ± 328	608 ± 185
Fold change C_{testis}	1.0	2.9	1.7	6.5	1.3	1.0
Testis-to-plasma ratio	0.88 ± 0.29	2.11 ± 0.67*	1.28 ± 1.03	3.11 ± 0.65***	0.89 ± 0.49	1.37 ± 0.69
Fold change ratio	1.0	2.4	1.5	3.5	1.0	1.6
P_{testis} (*10^{-3} h^{-1})	77.3 ± 24.2	180.8 ± 26.3**	102.9 ± 90.1	248.9 ± 29.8***	73.7 ± 28.4	98.3 ± 34.8
Fold change P_{testis}	1.0	2.3	1.3	3.2	1.0	1.3

Data are presented as mean ± S.D. (n = 6–9). $AUC_{0\text{-}8h}$, area under the plasma concentration-time curve; C_{max}, maximum concentration in plasma; T_{max}, time point (h) of maximum plasma concentration; $C_{brain/testis}$, brain/testis concentration; $P_{brain/testis}$, brain/testis accumulation, calculated by determining the brigatinib brain/testis concentration relative to the $AUC_{0\text{-}8h}$. *, $P < 0.05$; **, $P < 0.01$; ***, $P < 0.001$ compared to wild-type mice. #, $P < 0.05$; ##, $P < 0.01$; ###, $P < 0.001$ comparing *Abcb1a/1b*$^{-/-}$ and *Abcb1a/1b;Abcg2*$^{-/-}$ mice. ^, $P < 0.05$; ^^, $P < 0.01$ comparing *Cyp3a*$^{-/-}$ and Cyp3aXAV mice.

male wild-type and *Abcb1a/1b;Abcg2*$^{-/-}$ mice, and assessed plasma and brain brigatinib levels 4 h later. In vehicle-treated mice, the brigatinib plasma $AUC_{0\text{-}4h}$ was higher (1.4-fold) in *Abcb1a/1b;Abcg2*$^{-/-}$ mice compared to wild-type mice, but this was not significant (P = 0.07) given the high interindividual variation (Supplemental Figure 6; Table 2). Pretreatment with elacridar resulted in a 1.3-fold increase in brigatinib plasma $AUC_{0\text{-}4h}$ in wild-type mice which was also not statistically significant (P = 0.11). The plasma $AUC_{0\text{-}4h}$ in *Abcb1a/1b;Abcg2*$^{-/-}$ mice remained virtually unchanged (1.1-fold increase) by elacridar pretreatment, although it was borderline higher than that in vehicle-treated wild-type mice ($P < 0.05$, Table 2).

In the absence of elacridar, brain-to-plasma ratios were 38-fold higher in *Abcb1a/1b;Abcg2*$^{-/-}$ mice than in wild-type mice (Fig. 4A; Table 2). In contrast to the modest effects on plasma exposure, elacridar treatment dramatically increased the brain-to-plasma ratios of brigatinib in wild-type mice by 36-fold (Fig. 4A, C; Table 2), *i.e.*, to levels similar to those observed in *Abcb1a/1b;Abcg2*$^{-/-}$ mice with or without elacridar (Fig. 4B; Table 2). Since brain-to-plasma ratios were not

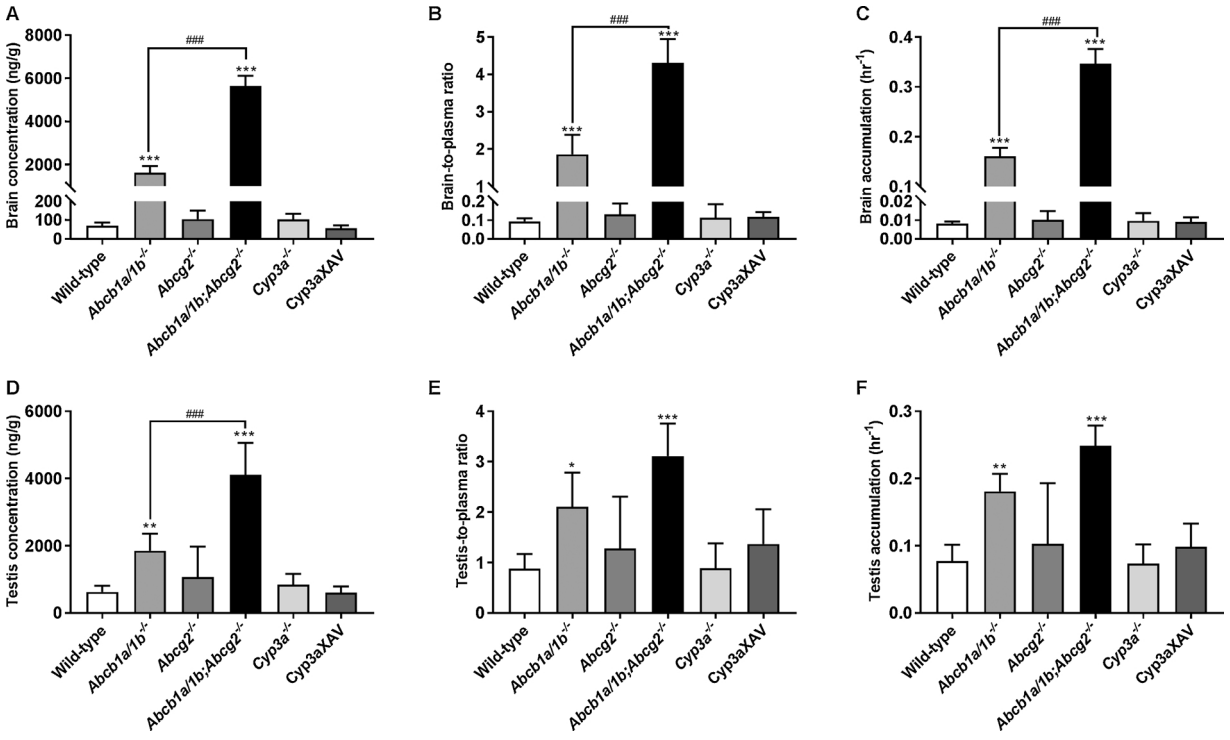

Fig. 3. Brain and testis concentration (A, D), tissue-to-plasma ratio (B, E), and tissue accumulation (C, F) of brigatinib in male wild-type, *Abcb1a/1b*$^{-/-}$, *Abcg2*$^{-/-}$, *Abcb1a/1b;Abcg2*$^{-/-}$, *Cyp3a*$^{-/-}$, and Cyp3aXAV mice 8 h after oral administration of 10 mg/kg brigatinib. Data are presented as mean ± S.D. (n = 6–9). *, $P < 0.05$; **, $P < 0.01$; ***, $P < 0.001$ compared to wild-type mice. #, $P < 0.05$; ##, $P < 0.01$; ###, $P < 0.001$ comparing *Abcb1a/1b*$^{-/-}$ with *Abcb1a/1b;Abcg2*$^{-/-}$ mice.

Table 2
Plasma, brain, and testis pharmacokinetic parameters of brigatinib 4 h after oral administration of 5 mg/kg brigatinib to male wild-type and *Abcb1a/1b;Abcg2*$^{-/-}$ mice with vehicle or elacridar coadministration.

Parameter	Genotype and type of pre-treatment			
	Vehicle		Elacridar	
	Wild-type	*Abcb1a/1b;Abcg2*$^{-/-}$	Wild-type	*Abcb1a/1b;Abcg2*$^{-/-}$
$AUC_{0\text{-}4h}$, ng/ml.h	2335 ± 839	3264 ± 895	3051 ± 685	3580 ± 247*
Fold increase $AUC_{0\text{-}4h}$	1.0	1.4	1.3	1.5
C_{max}, ng/ml	747.9 ± 281.5	892.1 ± 189.3	889.7 ± 173.0	1113.3 ± 162.5
T_{max}, h	1	4	2	4
C_{brain}, ng/g	40.8 ± 19.8	2329 ± 850***	1714 ± 333***	2937 ± 679***(^^)
Fold increase C_{brain}	1.0	57.1	42.0	72.0
Brain-to-plasma ratio	0.06 ± 0.01	2.29 ± 0.51***	2.17 ± 0.50***	2.60 ± 0.58***
Fold increase ratio	1.0	38.2	36.2	43.3
P_{brain} ($*10^{-3}$ h^{-1})	15.3 ± 2.5	642.5 ± 88.5***	532.8 ± 67.4***	759.0 ± 89.5***(#)^^^
Fold increase P_{brain}	1.0	42.0	34.8	49.6
C_{testis}, ng/g	169.0 ± 88.8	1147 ± 523***	1178 ± 261***	1424 ± 314***
Fold increase C_{testis}	1.0	6.8	7.0	8.4
Testis-to-plasma ratio	0.26 ± 0.05	1.10 ± 0.29***	1.49 ± 0.38***	1.27 ± 0.30***
Fold increase ratio	1.0	4.2	5.7	4.9
P_{testis} ($*10^{-3}$ h^{-1})	62.0 ± 13.9	307.4 ± 43.5***	367.8 ± 77.0***	368.3 ± 45.3***
Fold increase P_{testis}	1.0	5.0	5.9	5.9

Data are presented as mean ± S.D. (n = 7). Brigatinib was administered alone or coadministered with 50 mg/kg oral elacridar 15 min prior to brigatinib administration. $AUC_{0\text{-}4h}$, area under the plasma concentration-time curve; C_{max}, maximum concentration in plasma; T_{max}, time point (h) of maximum plasma concentration; $C_{brain/testis}$, brain/testis concentration; $P_{brain/testis}$, brain/testis accumulation. *, $P < 0.05$; **, $P < 0.01$; ***, $P < 0.001$ compared to vehicle-treated wild-type mice; #, $P < 0.05$ comparing *Abcb1a/1b;Abcg2*$^{-/-}$ mice with vehicle to elacridar. ^, $P < 0.05$; ^^, $P < 0.01$; ^^^, $P < 0.001$ comparing elacridar-treated wild-type mice to elacridar-treated *Abcb1a/1b;Abcg2*$^{-/-}$ mice.

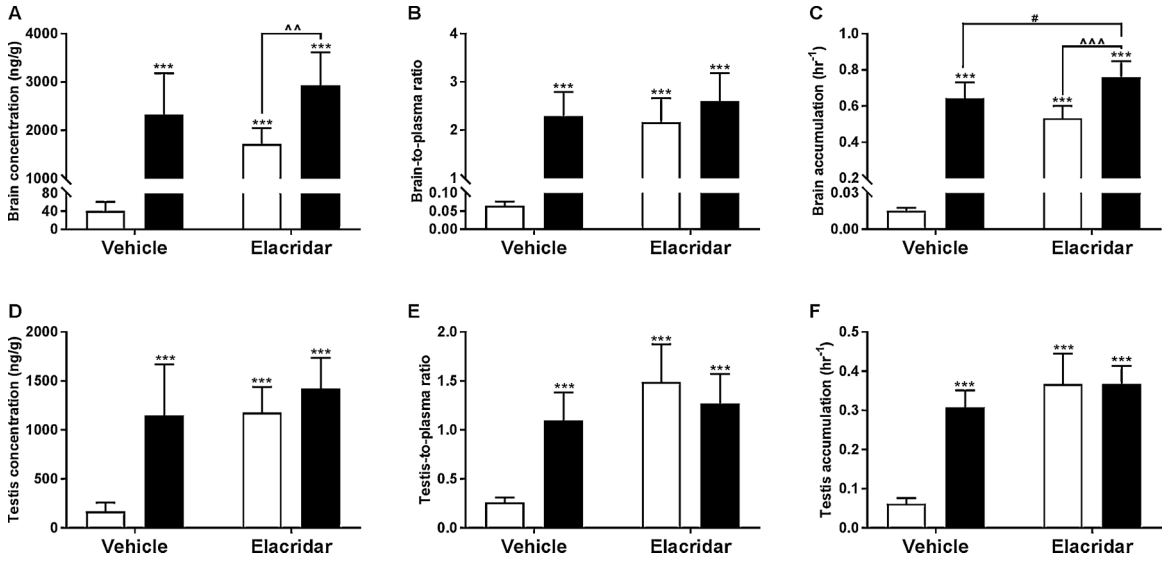

Fig. 4. Brain and testis concentrations (A, D), tissue-to-plasma ratios (B, E) and tissue accumulations (C, F) of brigatinib in male wild-type (white bars) and *Abcb1a/1b;Abcg2*$^{-/-}$ mice (black bars) 4 h after oral administration of 5 mg/kg brigatinib without or with oral elacridar (50 mg/kg) coadministration. Data are presented as mean ± S.D. (n = 7). *, $P < 0.05$; **, $P < 0.01$; ***, $P < 0.001$ compared to vehicle-treated wild-type mice; #, $P < 0.05$ comparing *Abcb1a/1b;Abcg2*$^{-/-}$ mice cotreated with either vehicle or elacridar. ^, $P < 0.05$; ^^, $P < 0.01$; ^^^, $P < 0.001$ comparing *Abcb1a/1b;Abcg2*$^{-/-}$ to wild-type mice both with elacridar coadministration.

markedly altered in the presence of elacridar in *Abcb1a/1b;Abcg2*$^{-/-}$ mice (Fig. 4A–C; Table 2), the pharmacokinetic effect of elacridar appears to be specifically mediated by the inhibition of mAbcb1a and mAbcg2 in the BBB.

Elacridar coadministration also resulted in a pronounced increase in the testis-to-plasma ratio of brigatinib in wild-type mice by 5.7-fold ($P < 0.001$), resulting in levels similar to those observed in *Abcb1a/1b;Abcg2*$^{-/-}$ mice with or without elacridar pretreatment (Fig. 4D–F; Table 2). In vehicle-treated mice, there were no significant differences between wild-type and *Abcb1a/1b;Abcg2*$^{-/-}$ mice in liver-to-plasma ratios of brigatinib, which could, however, be significantly increased by coadministration of elacridar in both strains (Supplemental Figure 7A-C). This suggests that elacridar might also inhibit some brigatinib elimination system in the liver other than Abcb1 and Abcg2, additionally boosting the liver accumulation of brigatinib. Something similar might apply to the lung although in this case elacridar did not significantly increase the lung-to-plasma ratio in *Abcb1a/1b;Abcg2*$^{-/-}$ mice (Supplemental Figure 7D-F). In contrast, the small intestinal tissue distribution of brigatinib was not noticeably affected by elacridar treatment in either mouse strain (Supplemental Figure 7G-I). Of note, toxicity signs similar to those seen previously were still observed in some vehicle-treated *Abcb1a/1b;Abcg2*$^{-/-}$ mice and in elacridar-

treated mice, including both wild-type and *Abcb1a/1b;Abcg2*$^{-/-}$ mice, even after we had reduced the dose of brigatinib to 5 mg/kg.

Collectively, these data indicate that oral elacridar pretreatment can extensively and specifically inhibit the activity of mouse Abcb1 and Abcg2 in the BBB and BTB, leading to profoundly increased brigatinib distribution to the brain and testis, and increased toxicity. The lack of effect of elacridar on the brain and testis accumulation in *Abcb1a/1b;Abcg2*$^{-/-}$ mice further suggests that other uptake or efflux systems for brigatinib across the BBB and BTB were not noticeably affected by elacridar at this dose (Fig. 4A–F; Table 2). However, in liver and lung potentially some other brigatinib clearing system(s) were affected (inhibited) by elacridar.

4. Discussion

This study shows that brigatinib is an excellent transport substrate of human ABCB1 and mouse Abcg2, and a good transport substrate of human ABCG2 *in vitro*. Accordingly, while single mAbcb1a/1b or mAbcg2 deficiency had no significant impact on the oral availability of brigatinib in mice, the combined deficiency resulted in a 1.9-fold increase in plasma $AUC_{0\text{-}8\,h}$. We further found dramatic increases in brigatinib brain accumulation in *Abcb1a/1b*$^{-/-}$ (19.3-fold) and *Abcb1a/1b;Abcg2*$^{-/-}$ mice (41.8-fold). These BBB transporters thus actively keep brigatinib out of the brain, with Abcb1a/1b playing a dominant role. Qualitatively similar effects were observed for brigatinib accumulation in testis. In contrast, brigatinib distribution to most other tissues was not noticeably affected by the transporter deficiencies. Elacridar coadministration could completely reverse the effect of Abcb1a/1b and Abcg2 in limiting brigatinib brain and testis accumulation. Unexpectedly, Abcb1 deficiency or pharmacological inhibition also resulted in highly increased acute toxicity of brigatinib, demonstrating an important protective role for this transporter. Brigatinib oral availability in mice was further restricted by mouse Cyp3a and even more by human CYP3 A4. This indicates that CYP3 A4 can play a substantial role in the metabolic clearance of brigatinib *in vivo*.

Similar to crizotinib and many other TKIs [15,16], brigatinib is a dual Abcb1a/1b and Abcg2 transport substrate, and *in vivo* subject to collaborative action of these proteins at the BBB. This is consistent with FDA registration documentation suggesting that brigatinib is transported by ABCB1 and ABCG2 *in vitro*. The phenomenon that single knockout of one of the transporters (in this case Abcg2) has no detectable effect on brain distribution of a drug, whereas in combination with the other transporter knockout it does have a clear effect, has previously been reported and explained using straightforward pharmacokinetic models [25,26]. In the case of brigatinib, Abcb1a/1b clearly has a more pronounced role than Abcg2 in restricting its brain penetration.

Considering the very limited brain penetration of brigatinib observed in wild-type mice at both the 10 and 25 mg/kg dosages, and its potential relevance for limiting therapeutic efficacy against brain metastases, we focused on ways to improve (boost) the brain concentration of brigatinib. To avoid additional toxicity from the elacridar coadministration, 5 mg/kg brigatinib and 50 mg/kg elacridar dosages were adopted in the boosting experiment. We demonstrated that virtually complete inhibition of the Abcb1 and Abcg2 transporters in the BBB could be achieved using a clinically realistic coadministration schedule. After further preclinical and clinical assessment, our finding could therefore potentially provide a rationale for improved treatment for brain metastases of ALK-positive lung cancer by enhancing brain penetration of brigatinib using oral coadministration of elacridar and brigatinib.

In the elacridar boosting experiment with 5 mg/kg oral brigatinib (Supplemental Figure 6; Table 2) there was a 1.4-fold increase in the plasma AUC between vehicle-treated wild-type and *Abcb1a/1b;Abcg2*$^{-/-}$ mice, but this was not statistically significant, whereas in the preceding 10 mg/kg oral brigatinib experiment we observed a significant 1.9-fold increase (Fig. 2; Table 1). The relative impact of Abcb1a/1b and Abcg2 therefore appeared higher at the higher dose. This could for instance be because other (transport or metabolizing) systems limiting the oral availability of brigatinib get saturated at the higher brigatinib dose.

The lethal acute toxicity of brigatinib that we observed in mice in which Abcb1a/1b (and Abcg2) was absent or inhibited was unexpected. However, these toxicity symptoms were quite similar to those previously observed in Sprague Dawley rats receiving chronic, daily oral administration of brigatinib. Six out of 50 rats died between study days 35 and 49 showing tonic convulsions, labored respiration, and hypoactivity. Dried brown/red material around the nose, mouth and/or anogenital area were also observed in the rats [20].

The toxicity we observed did not relate directly to the plasma exposure of brigatinib, as the plasma exposure in *Cyp3a*$^{-/-}$ mice at 25 mg/kg brigatinib was at least as high as that in *Abcb1a/1b;Abcg2*$^{-/-}$ mice (Supplemental Fig. 2; Supplemental Table 1), and yet we did not observe any sign of toxicity in the *Cyp3a*$^{-/-}$ mice. The pronounced difference in susceptibility, also considering the modest effects on tissue distribution of brigatinib in the Abcb1a/1b knockouts except for brain and testis, suggests that the highly increased CNS distribution of brigatinib is behind the lethal toxicity. Perhaps chronic administration as in the earlier rat study can lead to a toxic build-up of brigatinib in the CNS that happens much more quickly when Abcb1a/1b is absent or inhibited. However, we cannot exclude that some other, as yet unidentified, tissue compartment critical for the acute brigatinib toxicity is normally protected by Abcb1.

Given our toxicity results, any attempt to apply an efficacious ABCB1/ABCG2 inhibitor in patients in order to improve the CNS distribution of brigatinib, must be carefully monitored for increased toxicity symptoms. In fact, if humans would respond similarly to mice in developing toxicity when blocking ABCB1 function during brigatinib treatment, it may be impossible to safely apply this principle in patients. Insights from the current study may thus be helpful in deciding on what strategies to pursue (or not) in further improving the therapeutic efficacy of brigatinib.

In the *in vitro* transepithelial transport experiments, there was still some apically directed transport of brigatinib in all the MDCK-II cell lines, even with ABCB1 and/or ABCG2 inhibitors present (Fig. 1B, D, F, and H). Although small, these effects suggest that there is some other, modest, apically directed efflux transporter for brigatinib in MDCK-II cells. Interestingly, in the elacridar boosting experiment, we observed a marked increase in the liver distribution of brigatinib compared with the vehicle-treated mice in both wild-type and *Abcb1a/1b;Abcg2*$^{-/-}$ mice (Supplemental Figure 6). This result would be compatible with the existence of a bile canalicular efflux protein for brigatinib other than Abcb1 and Abcg2 that could be inhibited by elacridar, thus causing the higher accumulation of brigatinib in the liver. The nature of such a putative transport protein is currently unclear, but it is unlikely to be Abcc2, given the inhibition by elacridar [27].

According to the FDA documentation, brigatinib is primarily metabolized by CYP2C8 and CYP3 A4 *in vitro* [20]. However, to date, very limited information is publicly available on to what extent brigatinib interacts with CYP3 A *in vivo*. A substantial increase in plasma exposure was observed in *Cyp3a*$^{-/-}$ mice (1.5-fold, $P < 0.001$) with oral administration of 25 mg/kg brigatinib compared to wild-type mice. However, at 10 mg/kg, no statistically significant difference was observed in the $AUC_{0\text{-}8h}$ between *Cyp3a*$^{-/-}$ and wild-type mice, even though this is still 1.3-fold higher in the *Cyp3a*$^{-/-}$ mice. These results suggest that some enzymes, possibly including mouse Cyp2c isoforms, also participated in primary metabolism of brigatinib. Such enzymes may have been saturated by the higher brigatinib dose (25 mg/kg), resulting in a better discernible effect of the mouse Cyp3a isoform(s) in restricting the systemic exposure of brigatinib. It is worth noting that intestinal and hepatic human CYP3 A4 can substantially reduce the oral availability and thus overall body exposure of brigatinib, as judged by

comparing the $AUC_{0\text{-}8h}$ in Cyp3aXAV and *Cyp3a*$^{-/-}$ mice. This clearly suggests that the metabolic clearance and oral availability of brigatinib will also be noticeably affected by CYP3 A activity in humans, which is in line with the FDA documentation suggesting caution (and dose adjustment) during coadministration of brigatinib with strong CYP3 A inhibitors and inducers.

To the best of our knowledge, this is the first study documenting that in mice Abcb1a/1b and Abcg2 together restrict brigatinib brain accumulation and oral availability, with Abcb1a/1b playing the dominant role in limiting brain accumulation. Furthermore, human CYP3 A4 can substantially limit the oral availability of brigatinib, without altering its relative tissue distribution. Coadministration of elacridar could markedly improve the brain and testis accumulation of oral brigatinib without substantially altering systemic exposure, but clear toxicities were observed in some elacridar-treated mice. The obtained insights and principles may be used to cautiously try and enhance the therapeutic application, efficacy and safety of brigatinib, especially when considering treatment of brain metastases in NSCLC patients.

Conflict of interest

The research group of Alfred H. Schinkel receives revenue from commercial distribution of some of the mouse strains used in this study. The remaining authors declare no conflict of interest.

Financial support

This work was funded in part by the China Scholarship Council (CSC Scholarship No. 201606220081).

Appendix A. Supplementary data

Supplementary material related to this article can be found, in the online version, at doi:10.1016/j.phrs.2018.09.020.

References

[1] R.L. Siegel, K.D. Miller, A. Jemal, Cancer statistics, 2018, CA: Cancer J. Clin. 68 (2018) 7–30.
[2] M. Soda, Y.L. Choi, M. Enomoto, S. Takada, Y. Yamashita, S. Ishikawa, et al., Identification of the transforming EML4-ALK fusion gene in non-small-cell lung cancer, Nature 448 (7153) (2007) 561–566.
[3] E.L. Kwak, Y.J. Bang, D.R. Camidge, A.T. Shaw, B. Solomon, R.G. Maki, et al., Anaplastic lymphoma kinase inhibition in non-small-cell lung cancer, New Engl. J. Med. 363 (18) (2010) 1693–1703.
[4] G. Toyokawa, T. Seto, Updated evidence on the mechanisms of resistance to ALK inhibitors and strategies to overcome such resistance: clinical and preclinical data, Oncol. Res. Treat. 38 (6) (2015) 291–298.
[5] D.B. Costa, A.T. Shaw, S.H. Ou, B.J. Solomon, G.J. Riely, M.J. Ahn, et al., Clinical experience with crizotinib in patients with advanced ALK-rearranged non-small-cell lung cancer and brain metastases, J. Clin. Oncol. 33 (17) (2015) 1881–1888.
[6] A.T. Shaw, L. Gandhi, S. Gadgeel, G.J. Riely, J. Cetnar, H. West, et al., Alectinib in ALK-positive, crizotinib-resistant, non-small-cell lung cancer: a single-group, multicentre, phase 2 trial, Lancet Oncol. 17 (2) (2016) 234–242.
[7] L. Crino, M.J. Ahn, F. De Marinis, H.J. Groen, H. Wakelee, T. Hida, et al., Multicenter phase II study of whole-body and intracranial activity with ceritinib in patients with ALK-rearranged non-small-cell lung cancer previously treated with chemotherapy and crizotinib: results from ASCEND-2, J. Clin. Oncol. 34 (24) (2016) 2866–2873.
[8] W.S. Huang, S. Liu, D. Zou, M. Thomas, Y. Wang, T. Zhou, et al., Discovery of brigatinib (AP26113), a phosphine oxide-containing, potent, orally active inhibitor of anaplastic lymphoma kinase, J. Med. Chem. 59 (10) (2016) 4948–4964.
[9] S. Zhang, R. Anjum, R. Squillace, S. Nadworny, T. Zhou, J. Keats, et al., The Potent ALK inhibitor brigatinib (AP26113) overcomes mechanisms of resistance to first- and second-generation alk inhibitors in preclinical models, Clin. Cancer Res. 22 (22) (2016) 5527–5538.
[10] D.W. Kim, M. Tiseo, M.J. Ahn, K.L. Reckamp, K.H. Hansen, S.W. Kim, et al., Brigatinib in patients with crizotinib-refractory anaplastic lymphoma kinase-positive non-small-cell lung cancer: a randomized, multicenter phase II trial, J. Clin. Oncol. (2017) Jco2016715904.
[11] S.N. Gettinger, L.A. Bazhenova, C.J. Langer, R. Salgia, K.A. Gold, R. Rosell, et al., Activity and safety of brigatinib in ALK-rearranged non-small-cell lung cancer and other malignancies: a single-arm, open-label, phase 1/2 trial, Lancet Oncol. 17 (12) (2016) 1683–1696.
[12] P. Borst, R.O. Elferink, Mammalian ABC transporters in health and disease, Annu. Rev. Biochem. 71 (2002) 537–592.
[13] S. Agarwal, A.M. Hartz, W.F. Elmquist, B. Bauer, Breast cancer resistance protein and P-glycoprotein in brain cancer: two gatekeepers team up, Curr. Pharm. Des. 17 (26) (2011) 2793–2802.
[14] A.H. Schinkel, J.W. Jonker, Mammalian drug efflux transporters of the ATP binding cassette (ABC) family: an overview, Adv. Drug Deliv. Rev. 55 (1) (2003) 3–29.
[15] S.C. Tang, L.N. Nguyen, R.W. Sparidans, E. Wagenaar, J.H. Beijnen, A.H. Schinkel, Increased oral availability and brain accumulation of the ALK inhibitor crizotinib by coadministration of the P-glycoprotein (ABCB1) and breast cancer resistance protein (ABCG2) inhibitor elacridar, Int. J. Cancer 134 (6) (2014) 1484–1494.
[16] A. Kort, R.W. Sparidans, E. Wagenaar, J.H. Beijnen, A.H. Schinkel, Brain accumulation of the EML4-ALK inhibitor ceritinib is restricted by P-glycoprotein (P-GP/ABCB1) and breast cancer resistance protein (BCRP/ABCG2), Pharmacol. Res. 102 (2015) 200–207.
[17] W. Li, R.W. Sparidans, Y. Wang, M.C. Lebre, E. Wagenaar, J.H. Beijnen, et al., P-glycoprotein (MDR1/ABCB1) restricts brain accumulation and cytochrome P450-3A (CYP3A) limits oral availability of the novel ALK/ROS1 inhibitor lorlatinib, Int. J. Cancer 143 (8) (2018) 2029–2038.
[18] P.R. Lockman, R.K. Mittapalli, K.S. Taskar, V. Rudraraju, B. Gril, K.A. Bohn, et al., Heterogeneous blood-tumor barrier permeability determines drug efficacy in experimental brain metastases of breast cancer, Clin. Cancer Res. 16 (23) (2010) 5664–5678.
[19] K.S. Taskar, V. Rudraraju, R.K. Mittapalli, R. Samala, H.R. Thorsheim, J. Lockman, et al., Lapatinib distribution in HER2 overexpressing experimental brain metastases of breast Cancer, Pharm. Res. 29 (3) (2011) 770–781.
[20] FDA. Center for Drug Evaluation and Research of the US Department of Health and Human Service, Food and Drug Administration. Multi-discipline Review. Available from: https://www.accessdata.fda.gov/drugsatfda_docs/nda/2017/208772Orig1s000MultidisciplineR.pdf. 2017.
[21] K. Thelen, J.B. Dressman, Cytochrome P450-mediated metabolism in the human gut wall, J. Pharm. Pharmacol. 61 (5) (2009) 541–558.
[22] R. Evers, M. Kool, L. van Deemter, H. Janssen, J. Calafat, L.C. Oomen, et al., Drug export activity of the human canalicular multispecific organic anion transporter in polarized kidney MDCK cells expressing cMOAT (MRP2) cDNA, J. Clin. Invest. 101 (7) (1998) 1310–1319.
[23] E. Bakos, R. Evers, G. Calenda, G.E. Tusnady, G. Szakacs, A. Varadi, et al., Characterization of the amino-terminal regions in the human multidrug resistance protein (MRP1), J. Cell. Sci. 113 (Pt 24) (2000) 4451–4461.
[24] R.W. Sparidans, W. Li, A.H. Schinkel, J.H.M. Schellens, J.H. Beijnen, Bioanalytical liquid chromatography-tandem mass spectrometric assay for the quantification of the ALK inhibitors alectinib, brigatinib and lorlatinib in plasma and mouse tissue homogenates, J. Pharm. Biomed. Anal. 161 (2018) 136–143 (.).
[25] J.C. Kalvass, G.M. Pollack, Kinetic considerations for the quantitative assessment of efflux activity and inhibition: implications for understanding and predicting the effects of efflux inhibition, Pharm. Res. 24 (2) (2007) 265–276.
[26] H. Kodaira, H. Kusuhara, J. Ushiki, E. Fuse, Y. Sugiyama, Kinetic analysis of the cooperation of P-glycoprotein (P-gp/Abcb1) and breast cancer resistance protein (Bcrp/Abcg2) in limiting the brain and testis penetration of erlotinib, flavopiridol, and mitoxantrone, J. Pharmacol. Exp. Ther. 333 (3) (2010) 788–796.
[27] R. Evers, M. Kool, A.J. Smith, L. van Deemter, M. de Haas, P. Borst, Inhibitory effect of the reversal agents V-104, GF120918 and Pluronic L61 on MDR1 Pgp-, MRP1- and MRP2-mediated transport, Br. J. Cancer 83 (3) (2000) 366–374.